Pergamon

Solid State Communications, Vol. 101, No. 1, pp. 33–37, 1997

0038–1098/97 $17.00+.00

PII: S0038–1098(96)00546-7

MICROHARDNESS OF POROUS SILICON FILMS AND COMPOSITES

S.P. Duttagupta,[a] X.L. Chen,[b] S.A. Jenekhe[b] and P.M. Fauchet[c]

[a] Department of Electrical Engineering, University of Rochester, Rochester, NY 14627, U.S.A.
[b] Department of Chemical Engineering, University of Rochester, Rochester, NY 14627, U.S.A.
[c] Department of Electrical Engineering, Department of Physics & Astronomy and the Institute of Optics, University of Rochester, Rochester, NY 14627, U.S.A.

(*Received* 30 *July* 1996; *accepted* 10 *September* 1996 *by D.J. Lockwood*)

Microhardness measurements have been performed on porous silicon (PSi) films. The dependence of the hardness on porosity, morphology and the underlying silicon substrate has been established. A model which determines the intrinsic film hardness has been developed and experimentally validated. The load dependence of hardness was measured as an index of the disorder in porous silicon. Hardness analysis also provided information on the nature of the PSi surface. Finally, several PSi-polymer nanocomposites have been fabricated and characterized. An improvement in hardness is observed, with no apparent change in the PL characteristics. Copyright © 1996 Elsevier Science Ltd

Porous silicon (PSi) has been the focus of an intense research activity [1]. Most of the investigations to date have been primarily concerned with the optical properties of light-emitting porous silicon (LEPSi). However, for device fabrication purposes, information concerning the mechanical properties of LEPSi is also required. In this work, we report microhardness measurements of PSi films of varying porosities and morphologies. Since the hardness is strongly influenced by the underlying substrate, a model based on the volume of mixtures is developed in order to determine the actual hardness of thin, high porosity samples. Analysis of the hardness data was performed in order to determine the degree of disorder of the LEPSi samples and also the nature of the surface. Our results indicated that in order to improve the life expectancy of LEPSi devices, a significant improvement in the hardness of LEPSi films may be required. Accordingly, we have fabricated and characterized different nanocomposites, by infiltrating the pores with polymers. An increase in the hardness was observed in each case, without affecting the PL intensity.

Single crystal, (1 0 0) oriented, p^- Si (5–15 Ω-cm) and p^+ Si (0.1–0.01 Ω-cm) substrates were selected for anodization. The Psi films were formed over a wide range of porosities (P). In the case of p^+ substrates, P increased with the applied current density. For p^- substrates, P increased with a decrease in the HF concentration.

The microhardness measurements were performed with a Tukon 300 BM microhardness indenter at ambient laboratory conditions. The Vickers test uses a square based pyramidal indenter with an apex of $\emptyset = 136°$ causing a diamond shaped indent on the surface. This leads to the following expression for hardness [2]:

$$H_V = 1.8544(\mathrm{P}_L.d^{-2}), \quad (1)$$

where d (mm) is the mean diagonal length of the diamond shaped indent and P_L (1 Kgf = 9.8 N) is the applied load. Individual hardness values were calculated as a mean over 3 identically prepared samples and ten indentations per sample. The indentation depth (D) for the Vickers test approximately equals $d/7$ [3, 4]. To avoid the influence of the underlying c-Si substrate, it is required that $D \leq t/10$ (t: film thickness) [3]. For an applied load of 0.49 N and a film thickness of 20 μm, the above criteria was satisfied for all porosities. For most practical applications however, where $t \approx 1$ μm, the contribution from the Si substrate on the apparent hardness of the film cannot be neglected. Also, since efficient light emission occurs only at high porosities, this effect is even more pronounced. In order to determine the intrinsic hardness of the film, this substrate contribution needs to be corrected for. A simple model based on "volume of mixtures" was proposed by Sargent *et al.* [5] to determine the effective hardness of a

bilayer material as shown below:

$$H_V^* = (H_{V1}V_1 + H_{V2}V_2)/(V_1 + V_2), \quad (2)$$

where H_V^* is effective hardness, H_1 and H_2 are the hardnesses of the two layers, t is the thickness of the top layer, V_1 and V_2 are the volumes of the respective layers within a hemisphere of diameter d. To test the validity of Equation 2, a 70% porous p^+ PSi film was used. The film thickness (t) was varied between 0.1 μm and 1 μm. The volumes V_1 and V_2 were calculated from (d) and (t) data and the hardnesses H_1 and H_2 are those of a 20 μm thick, 70% porous layer and that of c-Si. The predicted and measured hardness values were compared to test the validity of the above model.

For determining the load dependence of hardness (also known as indentation size effect, ISE), we measured (d) for identically prepared samples under varying loads (1 gf–100 gf). The Meyer parameter (n) which is a measure of ISE, was determined from the power law relationship between the applied load and the indentation diagonal [2].

$$P_L = K_L d^n. \quad (3)$$

A value of $n < 2$ indicates that the material is a ceramic (for c-Si, $n = 1.7$) [6] in which case an increase in load would cause a decrease in hardness [6].

It may be noted that because of a dimensionality problem, it is difficult to attribute any physical significance to the Meyer parameter. The approach of Fröhlich *et al.* [7], in analyzing the load-indent size relationship has been to adopt a power series expression:

$$P_L = a_0 + a_1 d + a_2 d^2 + a_3 d^3 ..... \quad (4)$$

The expression was then limited to two terms as follows:

$$P_L = a_1 d + a_2 d^2. \quad (5)$$

It has been suggested that the coefficient a_1 represents the energy per indentation surface area of a sample, while a_2 represents the energy per indentation induced volume of permanent deformation [8]. It follows that a_1 is a "surface property", and hence, may be useful as an indicator of the quality of the surface.

The polymers used for the fabrication of nanocomposites were polyethylene, polypropylene, polystyrene, polymethyl methacrylate, polyvinyl chloride and polyamide. These materials are all commercially available and have been extensively characterized [9]. Standard organic solvents such as toluene and xylene were used to dissolve the polymers. The concentration was quite dilute (2–3%) in order to prevent film formation on the surface due to pore-bridging. The PSi samples were left immersed in solution for a period of two to three days, thereby allowing sufficient time for the polymer molecules to diffuse into the pores. The final step before characterization was a brief toluene rinse to remove any residual film on the surface. The intrinsic hardness of the nanocomposites was then determined by applying Equation 2 (PSi film thickness ~2 μm). In order to verify that the polymers had infiltrated inside the film, the composites were partially etched in a CF_4/O_2 plasma. The hardness of the etched region was measured and compared to that of the unetched film.

For an applied load of 0.49 N, the hardness of (1 0 0) c-Si (H_0) was determined to be 11.5 GPa [10]. The variation of hardness with porosity is shown in Fig. 1 for p^- PSi and p^+ PSi films. The fitting of the data shows a $(1\text{-}P)^{2/3}$ dependence until at 75–80% porosities, a further decrease in hardness is noticeable. For the same porosity, the p^- films have a higher hardness than the p^+ samples. The influence of the substrate in hardness measurements for highly porous p^+ PSi film is shown in Fig. 2. Even for a 1 μm thick film, the apparent hardness is 60% greater than the actual value of 4.5 GPa. The predicted and measured data agree well except for very thin films. The Meyer parameter (n) was evaluated as a function of porosity for p^- and p^+ PSi films (Fig. 3). The surface energy team a_1 was determined by regression. In Fig. 4, we plot the variation of a_1 with porosity for p^- and p^+ PSi films. Figure 5 shows that the hardness of all the nanocomposite structures is improved compared to the as-anodized PSi film. The

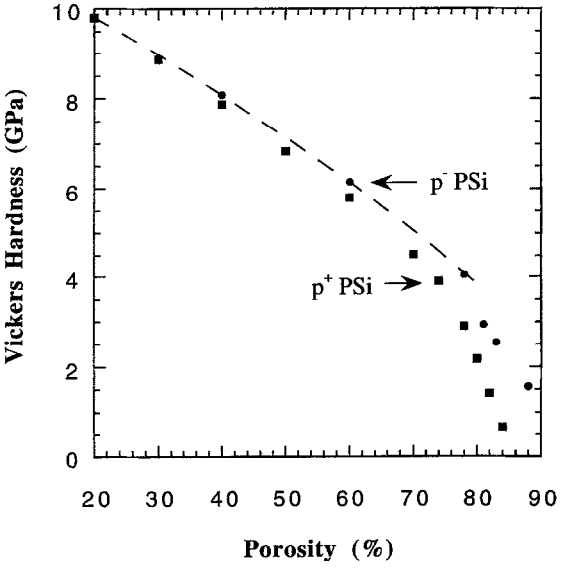

Fig. 1. Variation of hardness with film porosity formed on a p^- Si and p^+ Si substrate. For p^- films the J is 20 mA cm^{-2} and the HF concentration varies from 40% (P = 40%) to 20% (P = 88%). For p^+ films the HF concentration is 25% and J varies from 6 mA cm^{-2} (p = 20%) to 100 mA cm^{-2} (P = 84%). Applied load is 0.49 N. The dashed line follows the $(1\text{-}P)^{2/3}$ dependence.

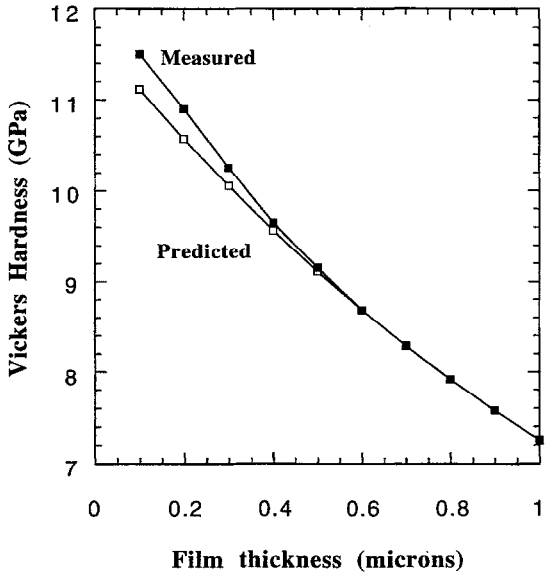

Fig. 2. Influence of the underlying Si substrate in the hardness measurements for high porosity PSi films. The 70% porosity PSi films were formed on a p^+ Si substrate. Applied load is 0.49 N.

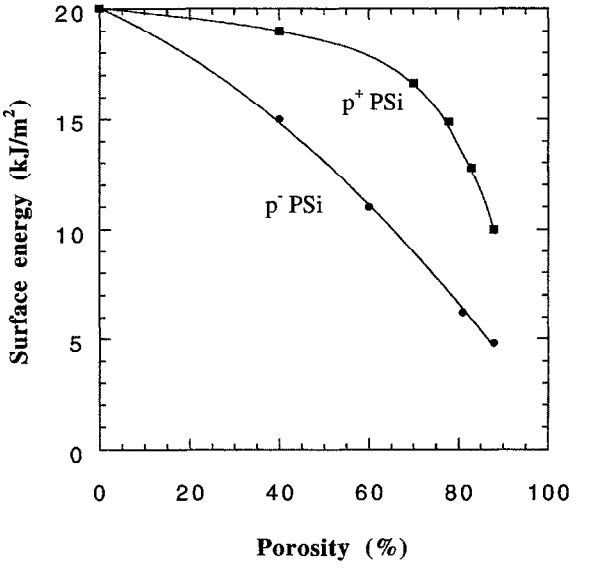

Fig. 4. Variation of surface energy (a_1) with porosity and substrate doping for films formed from p^- Si and p^+ Si substrate.

order of increase is polyethylene < polypropylene < PVC < polystyrene < PMMA < polyamide. The hardness of the partially etched films is similar to that of the unetched sample, indicating that the polymers have been able to penetrate the pores.

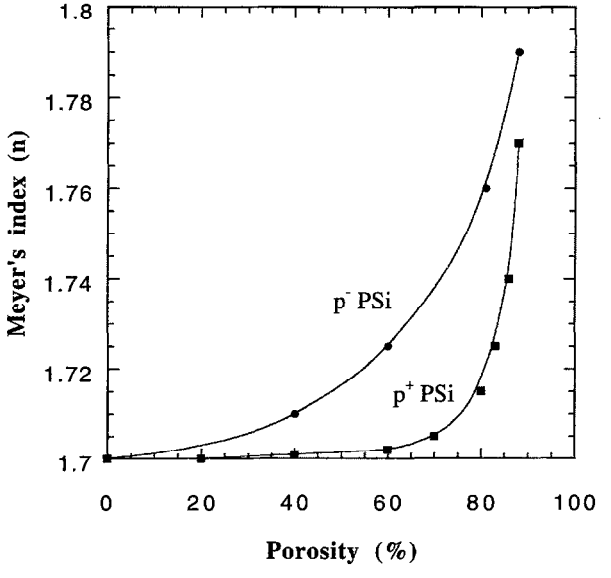

Fig. 3. Variation of Meyer's index (n) with porosity and substrate doping for films formed from p^- Si and p^+ Si substrate.

The hardness of a material is usually defined as the resistance to local deformation [5]. As seen in Fig. 1, the hardness for both p^- and p^+ PSi samples decreases with an increase in porosity. The proportionality factor is $(1\text{-P})^m$ ($m = 2/3$), which results in a more gradual decrease than the $(1\text{-}a\text{P-}b\text{P}^2)$ factor proposed for sintered materials [11]. A possible explanation for this is the highly crystalline structure of porous silicon even at high porosities [12]. Hardness is also affected by the film morphology. For the same porosity, the hardness of the p^- films is greater than that of the p^+ films. This can be related to the grain size differences between p^- PSi (2–3 nm) and p^+ PSi (3–10 nm) as observed from X-ray diffraction [13] and Raman analysis [14]. Such an increase in hardness with a decrease in grain size has been also reported for nanocrystalline metals and alloys [15] and for polycrystalline ceramics [6].

At porosities of 70%–80%, the measured hardness deviates from the $(1\text{-P})^{2/3}$ proportionality. This lends support to the small-angle scattering X-ray analyses of LEPSi [16] which indicated a large increase in pore size at high porosities, as the columns become stand-alone structures and pores coalesce. An increase in surface area results in a decrease in hardness since hardness is inversely proportional to the contact area. Hardness data can thus be conveniently used to identify this transition regime.

The Meyer's index is seen to be a good measure of the deviation of porous silicon from ideal crystalline behavior. For crystalline Si, $n = 1.7$ while for amorphized (highly

disordered) Si, $n = 2.0$ [6]. Even at 80% porosity, n (p^- PSi) = 1.75 and n (p^+ PSi) = 1.72 respectively. This is a further indication of the ordered nature of PSi.

The decrease in the surface energy term a_1 at higher porosities may be due to the increased disorder in the samples. It is important to note that especially at low P, a_1 is more sensitive to a change in porosity than (n). This is reasonable to expect, since a_1 is a surface property which is affected even at very low porosities, while (n) is influenced by the bulk and the surface. The superior sensitivity of a_1 may prove to be useful as a measure of surface quality of thin films.

Our results indicate that the hardness of the nanoporous light emitting films is about an order lower than that of crystalline silicon. A significant improvement in the mechanical and thermal properties may occur, if it is possible to infiltrate and fill the pores. Recently, Halimaoui *et al.* have reported the UHV deposition of Ge and Si onto PSi resulting in a progressive coverage of the inner surface and finally pore-filling [17]. The reason for choosing polymers for forming nanocomposites is the diverse range of properties and functionalities that these materials possess [9]. The hardness of the polymer/PSi nanocomposites in Fig. 5 increases (except for PVC) with the density of the base polymers [9]. The photoluminescence intensity and peak position remained unchanged. This is probably due to the large bandgaps (absence of trap states) and low dielectric constants (2.3–3.6) of the polymers (no screening effect).

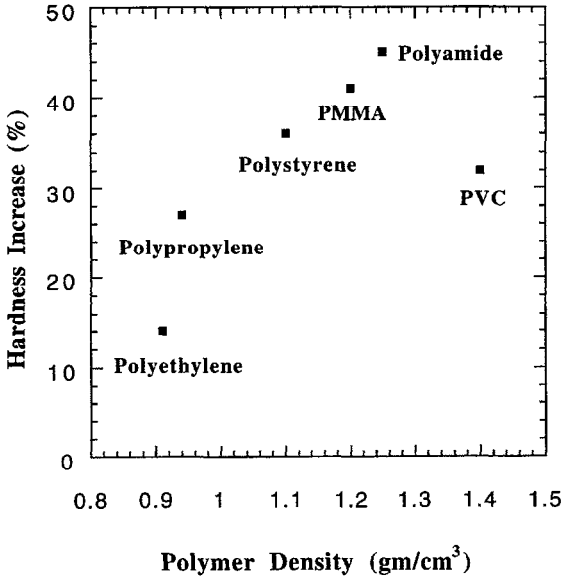

Fig. 5. Percentage increase in the hardness of LEPSi-polymer nanocomposites. The control sample is an as-anodized, 80% porous, p^+ film. Applied load is 0.49 N.

In conclusion, the hardness of porous silicon films and its variation with porosity and morphology are reported for the first time. The improvement in the hardness and other mechanical properties required for the fabrication of practical silicon based light emitters, may be achieved by forming nanocomposites with polymers. Preliminary results indicate that the hardness of nanocomposites is enhanced without affecting the optical properties of porous silicon. Further investigation of materials and process issues will be required in order to fabricate a composite with optimum mechanical, thermal, electrical and optical properties.

Acknowledgements—This work was supported by the NSF Science and Technology Center for Photoinduced Charge Transfer, NSF (CTS-9311741) and the Army Research Office. The authors wish to acknowledge the assistance of Birgit Puchebner of the Center for Optics Manufacturing at the University of Rochester, with the microindentation measurements.

REFERENCES

1. Fauchet, P.M., Tsybeskov, L., Peng, C., Duttagupta, S.P., von Behren, J., Kostoulas, Y., Vandyshev, J.V. and Hirschman, K.D., *IEEE Journ. Selec. Topics Quant. Elec.*, **1,** 1995, 1126.
2. Chicot, D. and Lesage, J., *Thin Solid Films*, **254,** 1995, 123.
3. Vingsbo, O., Hogmark, S., Jönsson, B. and Ingemarsson, A., *Microindentation Techniques in Materials Science and Engineering, ASTM STP 889* (Edited by P.J. Blau and B.R. Lawn), American Society for Testing and Materials, Philadelphia, 1986, pp. 257–271.
4. Tabor, D., *Microindentation Techniques in Materials Science and Engineering, ASTM STP 889* (Edited by P.J. Blau and B.R. Lawn), American Society for Testing and Materials, Philadelphia, 1986, pp. 129–159.
5. Sargent, P.M., *Microindentation Techniques in Materials Science and Engineering, ASTM STP 889* (Edited by P.J. Blau and B.R. Lawn), American Society for Testing and Materials, Philadelphia, 1986, pp. 160–174.
6. McColm, I.J., *Ceramic Hardness*, Plenum Press; New York, 1990.
7. Frohlich, F., Grau, P. and Grellmann, W., *Phys. Status Solidi A*, **42,** 1979, 79.
8. Li, H. and Bradt, R.C., *J. Noncryst. Sol.*, **146,** 1992, 197.
9. Brandrup, J. and Immergut, E.H., Editors, *The Polymer Handbook*, John Wiley and Sons, New York, 1975.
10. Ericson, F., Johansson, S. and Schweitz, J., *Mat. Sci. & Engg. A*, **105/106,** 1988, 131.
11. Mukhopadhyay, A.K., Datta, S.K. and Chakraborty, D., *Ceramics Inter.*, **17,** 1991, 121.

12. Barla, K., Herino, R., Bomchil, G., Pfister, J.C. and Freund, A., *J. Cryst. Growth,* **68,** 1984, 727.
13. Duttagupta, S.P. and Fauchet, P.M., to be published.
14. Münder, H., Berger, M.G., Frohnhoff, S., Thönissen, M. and Lüth, H., *Journ. Lum.*, **57,** 5, 1993.
15. Ganapathi, S.K. and Rigney, D.A., *Scripta Met. et Mater.*, **24,** 1990, 1675.
16. Vezin, V., Goudeau, P., Naudon, A., Halimaoui, A. and Bomchil, G., *Appl. Phys. Lett.*, **60,** 1992, 2625.
17. Halimaoui, A., Campidelli, Y., Badoz, P.A. and Bensahel, D., *J. Appl. Phys.*, **78,** 1995, 3428.